(Received 9 December 2025, Accepted 22 December 2025, Scheduled 13 January 2026)

Compact Wideband Antenna Design Incorporating DGS, Slots, and Tiny Reflectors for Wireless Applications

Nirav J. Chauhan[1, 2, *], Chandulal H. Vithalani[3], and Jagdish M. Rathod[4]

[1] Gujarat Technological University, Ahmedabad, Gujarat, India
[2] EC Department, Government Polytechnic, Palanpur, Gujarat, India
[3] EC Department, L.D. College of Engineering, Ahmedabad, Gujarat, India
[4] Department of Electronics, Birla Vishwakarma Mahavidyalaya, Vallabh Vidyanagar, Gujarat, India

ABSTRACT: To achieve wideband operation while maintaining a small overall footprint (26 mm × 27 mm × 1.6 mm) and electrical size of $0.46\lambda \times 0.47\lambda \times 0.03\lambda$, this paper presents a compact wideband Microstrip Patch Antenna (MPA) that uses a Defected Ground Structure (DGS) and internal slots on a radiating patch and ground plane. The proposed antenna was designed on FR-4 with loss tangent $= 0.02$, $\varepsilon_r = 4.4$ & $h = 1.6$ mm, which achieves a wide bandwidth covering key wireless bands (Sub-6 GHz 5G, Wi-Fi, WiMAX) with acceptable gain and radiation stability. The upper and lower edges of the band were tuned by the slot geometry and DGS, as demonstrated by parametric analysis. Full-wave electromagnetic simulation results are reported, and the fabrication and measurement procedure are described. The stated antenna achieves a peak radiation efficiency of 95.46%, a fractional bandwidth of 64.39%, a maximum gain of 4.8 dB, and an S_{11} below −10 dB over the range of frequency 3.57–6.96 GHz, all in a small size similar to a coin. The antenna is particularly suitable for compact wireless devices, IoT modules, and Sub-6 GHz applications.

1. INTRODUCTION

Compact wideband antennas are required for the latest wireless devices that support multiple bands (e.g., Wi-Fi, WiMAX, LTE, Sub-6 GHz) [1, 21–23]. Traditional patch antennas are compact and easy to fabricate but inherently narrowband. Techniques to broaden bandwidth include thick substrates, stacked patches, proximity coupling, and ground-plane modifications [16–20]. A compact single-layer approach combining slot loading and a patterned DGS is effective to increase the bandwidth while keeping the manufacturing simple [1, 14]. Adding slots to both the ground plane and the radiating element has been proven to help design small antennas that can operate over multiple frequency bands [11–13].

A compact patch antenna ($26 \times 27 \times 1.6\,\text{mm}^3$) with internal slots and an optimized DGS is presented. DGS offers an effective way to enhance antenna characteristics without complex multilayer fabrication and increasing antenna size.

2. MATHEMATICAL MODEL

The core mathematical formulations governing the MPA design are systematically outlined below:

Effective electrical length at resonance:

$$L_{ef} = \frac{c}{2f_r\sqrt{\varepsilon_{ef}}} \tag{1}$$

The extension length Δl:

$$\Delta l = 0.412h\,\frac{(\varepsilon_{ef}+0.300)\left(\frac{W}{h}+0.264\right)}{(\varepsilon_{ef}-0.258)\left(\frac{W}{h}+0.800\right)} \tag{2}$$

Physical patch length:

$$L = L_{ef} - 2\Delta l \tag{3}$$

Patch Width (W):

$$W = \frac{c}{2fr\sqrt{\frac{(\varepsilon_r+1)}{2}}} \tag{4}$$

Effective Permittivity (ε_{ef}):

$$\varepsilon_{ef} = \frac{(\varepsilon_r+1)}{2} + \frac{(\varepsilon_r-1)}{2}\left[1+\frac{12h}{w}\right]^{-1/2} \tag{5}$$

$$L_g = 6h + L \tag{6}$$

$$W_g = 6h + W \tag{7}$$

$$\eta_t = \eta_r \times \left(1 - |S_{11}|^2\right) \tag{8}$$

Equations (6) and (7) were used to determine the dimensions of the ground plane [2, 23].

3. PROPOSED ANTENNA DESIGN

Figure 1 shows the structural layout and dimensional specifications of the designed antenna. The antenna is compact, with dimensions of 26 mm × 27 mm × 1.6 mm.

* Corresponding author: Nirav Jashvantkumar Chauhan (niravjchauhan.ec@gmail.com).

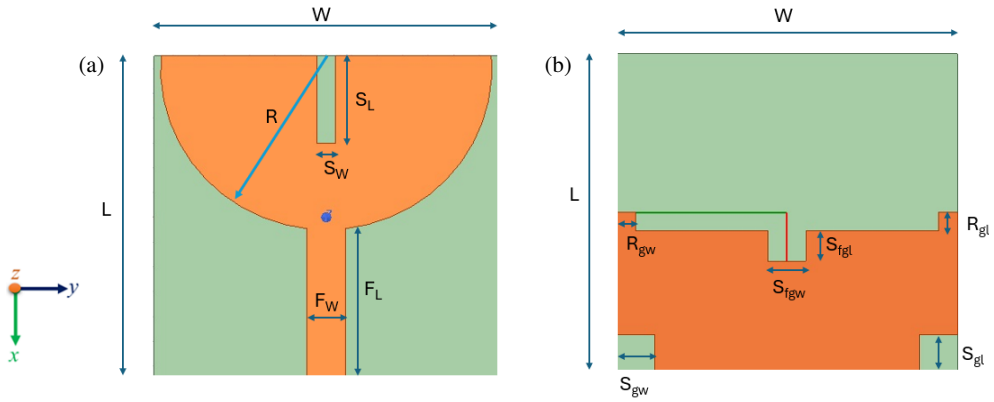

FIGURE 1. Optimized design of antenna: (a) Top view, (b) bottom view.

The antenna employs longitudinal symmetry, configured in the plane (x-y). The structure consists of a central radiating semicircular patch with radius (R) and slot at the center (S_L, S_W). A microstrip feed line, with length (F_L) and width (F_W), is implemented on the upper part of a dielectric substrate.

A DGS (defected ground structure) is etched into the bottom layer of the substrate to improve the key performance parameters, radiation gain, bandwidth (BW), and suppression of cross-polarization components [4, 15, 17].

The ground plane incorporates two identical tiny reflectors (R_{gl} and R_{gw}) for gain improvement. A rectangular slot (S_{fgl} and S_{fgw}) is introduced to achieve impedance matching, while two additional square slots (S_{gl}, S_{gw}) are incorporated to enhance the S_{11} performance. The electrical dimensions of the antenna are $0.46\lambda \times 0.47\lambda \times 0.03\lambda$. The detailed structural parameters are listed in Table 1.

TABLE 1. Detailed specification of the design parameters.

Parameter	Value	Parameter	Value
L	0.46λ	R	0.23λ
W	0.47λ	R_{gl}	0.02λ
h	0.03λ	R_{gw}	0.02λ
S_L	0.12λ	S_{gl}	0.05λ
S_W	0.02λ	S_{gw}	0.05λ
F_L	0.23λ	S_{fgl}	0.07λ
F_W	0.05λ	S_{fgw}	0.05λ

4. ANTENNA DESIGN EVOLUTION AND PERFORMANCE PARAMETER ANALYSIS

As illustrated in Figure 2, the antenna geometry was systematically modified to enhance wideband performance. Earlier research has shown that E-shaped and U-shaped patch antennas exhibit superior wideband characteristics. Accordingly, Antenna 1 was designed as a compact U-shaped configuration with a full ground plane. In Antenna 2, a centrally symmetrical slot was introduced within the U-shaped patch, and the ground was partially etched to further improve the impedance bandwidth. Antenna 3 incorporates two identical miniature reflectors on the ground plane to enhance the gain, along with a slot near the feedline to achieve better impedance matching. Finally, in Antenna 4, two identical slots are etched in the DGS of Antenna 3 to further extend the bandwidth. This progressive geometrical evolution results in a significant improvement in the impedance characteristics and a substantial enhancement in the overall wideband performance.

Figure 3 shows S_{11} variation with respect to frequency for antennas Design-1, 2, 3, and 4. -10 dB is considered as the reference line here. For wideband performance, a design that provides a wide S_{11} below -10 dB is considered good. Initially for Design-1, the S_{11} curve does not fall below -10 dB, so it is to be modified. With the first structural enhancement as mentioned in Design-2, an additional resonance emerges, and the S_{11} graph deepens significantly, indicating improved impedance matching, but it does not stay below -10 dB for the wideband. Further, geometric evolution, as mentioned in Design-3, introduces a wider bandwidth. In the final configuration, as mentioned in Design-4, the S_{11} graph is below -10 dB for bandwidth 3.57 to 6.96 GHz, which clearly indicates wideband performance due to the cumulative design enhancements.

Figure 4 shows that varying the Patch Slot Length (S_L) significantly affects the return loss of the antenna. The parametric analysis of S_L varying from 5 mm to 9 mm provided optimal performance at $S_L = 7$ mm; therefore, it was considered in the design.

As depicted in Figure 5, incorporating DGS (Defected Ground Structure) significantly affects S_{11} to a great extent. From Figure 5, it is clear that a ground plane between 40% and 50% improves the wideband characteristics; therefore, a ground plane with a size of 44.23% was taken into consideration in the design.

Figure 6 illustrates the impact of variations in F_W, S_{gl}, and S_{gw} on return loss. As per the figure's parametric analysis of F_W, S_{gl}, and S_{gw}, good performance is achieved for the dimensions of 3 mm and 3.5 mm, while maintaining structural symmetry. $F_W = S_{gl} = S_{gw} = 3$ mm dimensions are taken into the design consideration.

Figure 7 shows the impact of variations in S_W, R_{gl}, and R_{gw} on return loss. As per the parametric analysis of S_W, R_{gl}, and

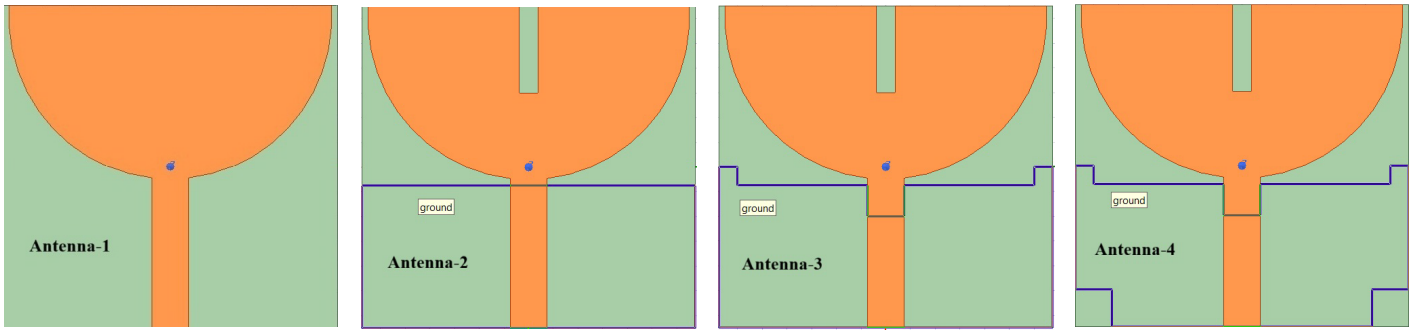

FIGURE 2. Progressive evaluation of antenna.

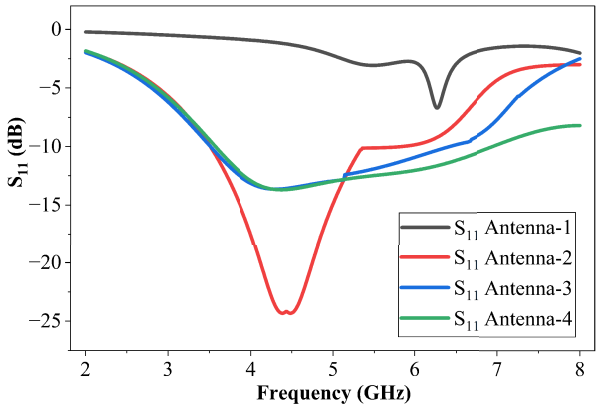

FIGURE 3. S_{11} variation across diverse designs.

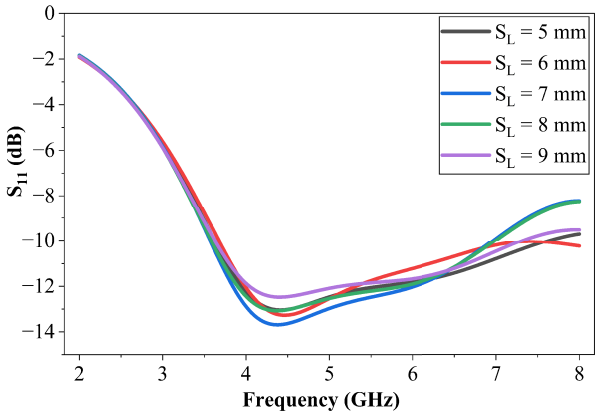

FIGURE 4. Parametric analysis: S_{11} variation as a function of patch slot length (S_L).

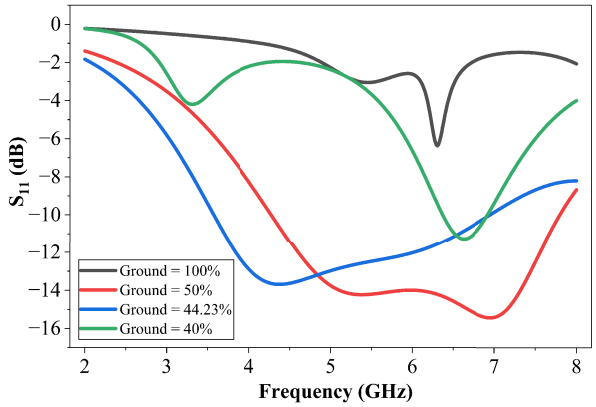

FIGURE 5. Parametric analysis: S_{11} variation as a function of the ground plane.

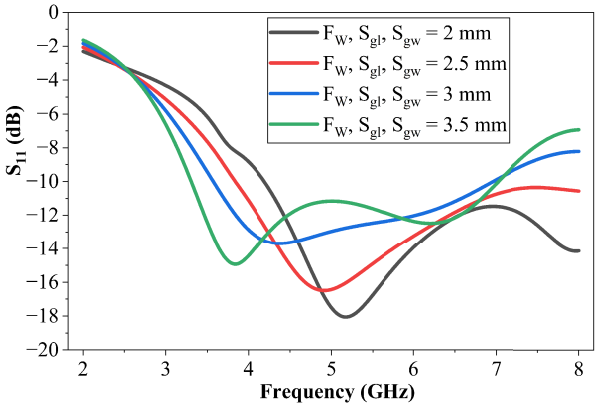

FIGURE 6. Parametric analysis: S_{11} variation as a function of feedline width (F_W), ground slot length (S_{gl}) and ground slot width (S_{gw}).

R_{gw}, the deepest resonance occurs at 1.5 mm, showing optimal performance. Therefore, $S_W = R_{gl} = R_{gw} = 1.5$ mm dimensions are considered in the design.

For structural symmetry and impedance matching, the Ground Feed Slot Width (S_{fgw}) is considered to be the same as the Feedline Width (F_W), which is equal to 3 mm. The Feedline Length (F_L) is taken as 13 mm, which is exactly the shortest distance between the periphery of the semi-circle of the patch and the excitation.

Figure 8 illustrates that varying the Ground Feed Slot Length (S_{fgl}) affects the S_{11} plot, and it is varied from 3 to 5 mm with a 0.5 mm interval as per the figure, and the overall geometry $S_{fgl} = 4$ mm is considered in the design.

5. RESULTS AND DISCUSSION

Figure 9 shows that our antenna prototype was simulated using ANSYS HFSS software.

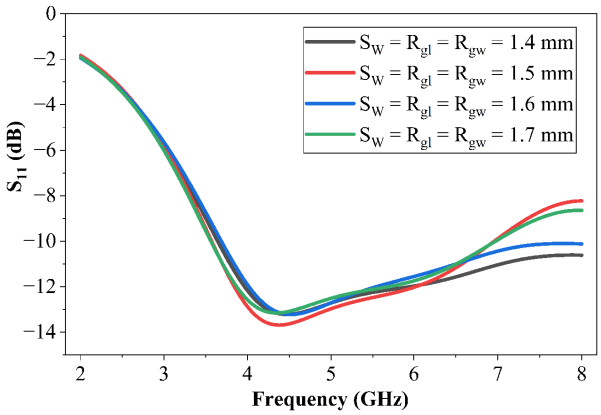

FIGURE 7. Parametric analysis: S_{11} variation as a function of patch slot width (S_W), ground reflector length (R_{gl}) and ground reflector width (R_{gw}).

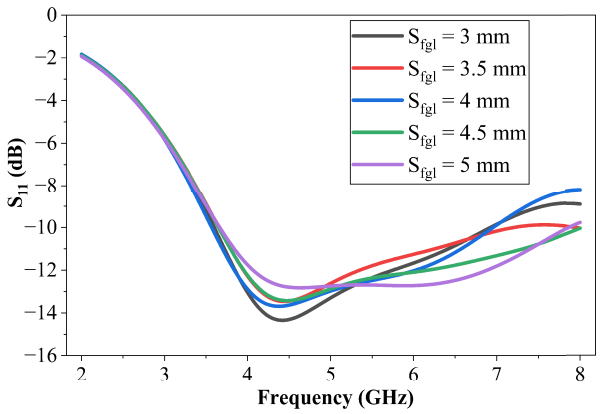

FIGURE 8. Parametric analysis: S_{11} variation as a function of ground feed slot length (S_{fgl}).

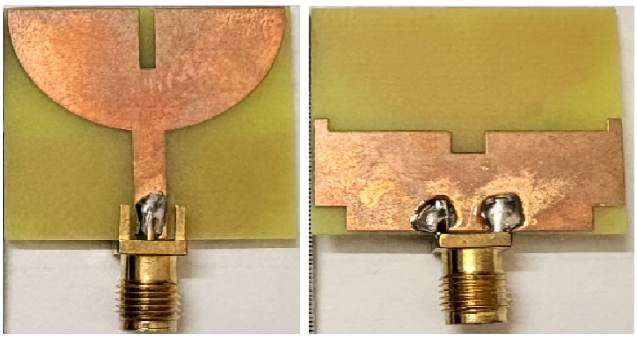

FIGURE 9. Antenna prototype.

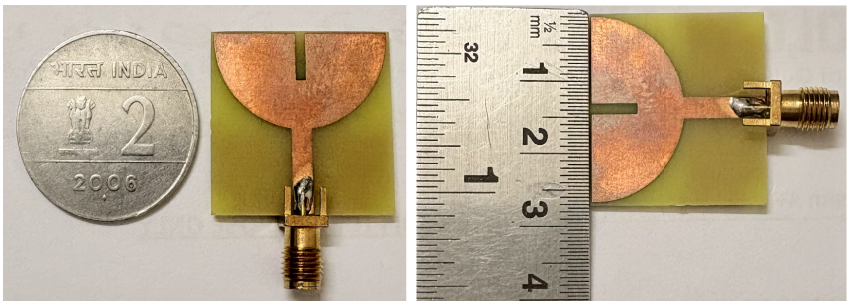

FIGURE 10. Compactness of proposed antenna — Dimension comparison.

(a) (b) (c)

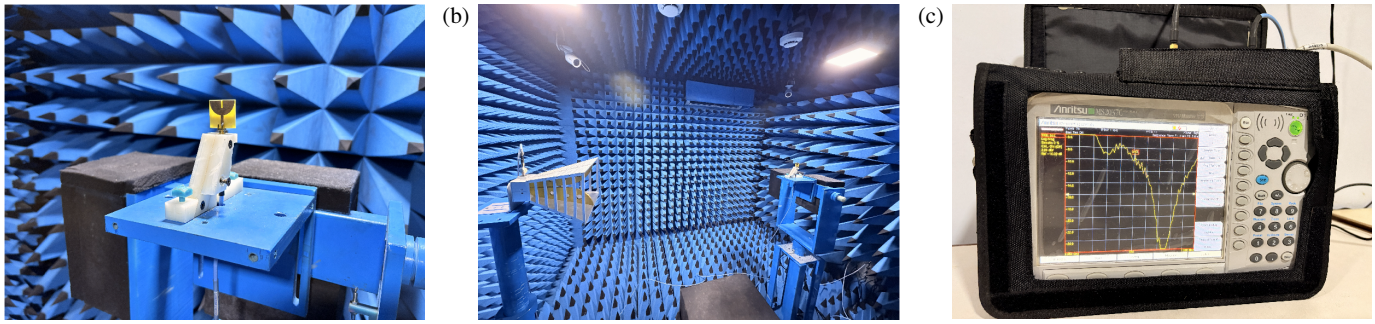

FIGURE 11. (a), (b) Measurement setup inside an ELARC anechoic chamber and (c) measurement with VNA.

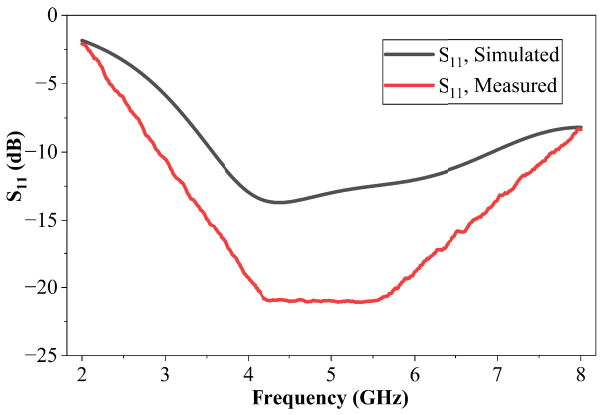

FIGURE 12. S_{11} parameter: simulated vs. measured results.

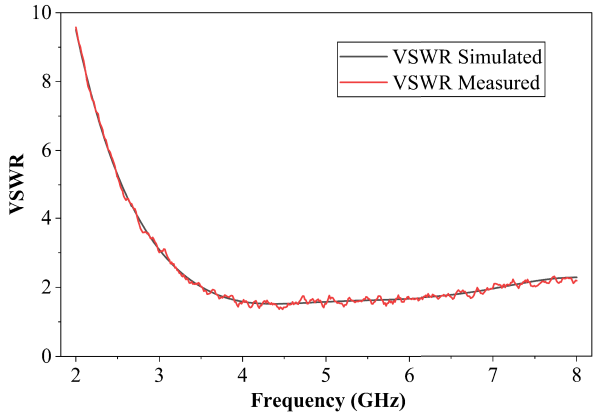

FIGURE 13. VSWR performance: simulated vs. measured results.

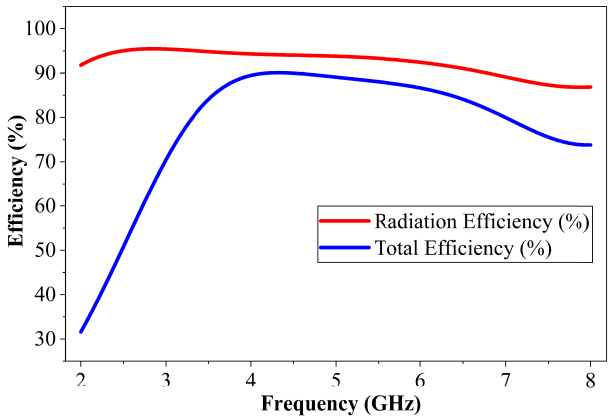

FIGURE 14. Radiation and total efficiency.

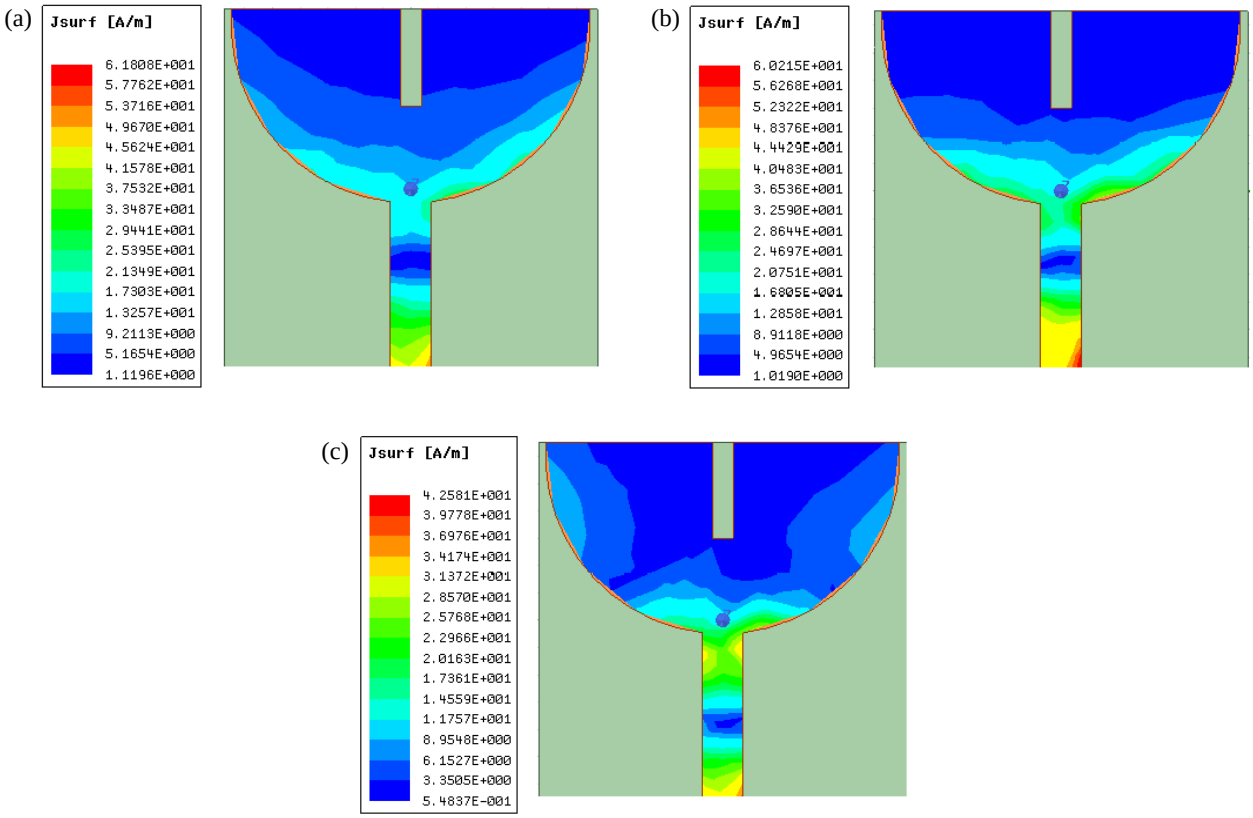

FIGURE 15. Analysis of the current distribution of the proposed antenna at frequencies (a) 4.2 GHz, (b) 5.7 GHz, (c) 6.9 GHz.

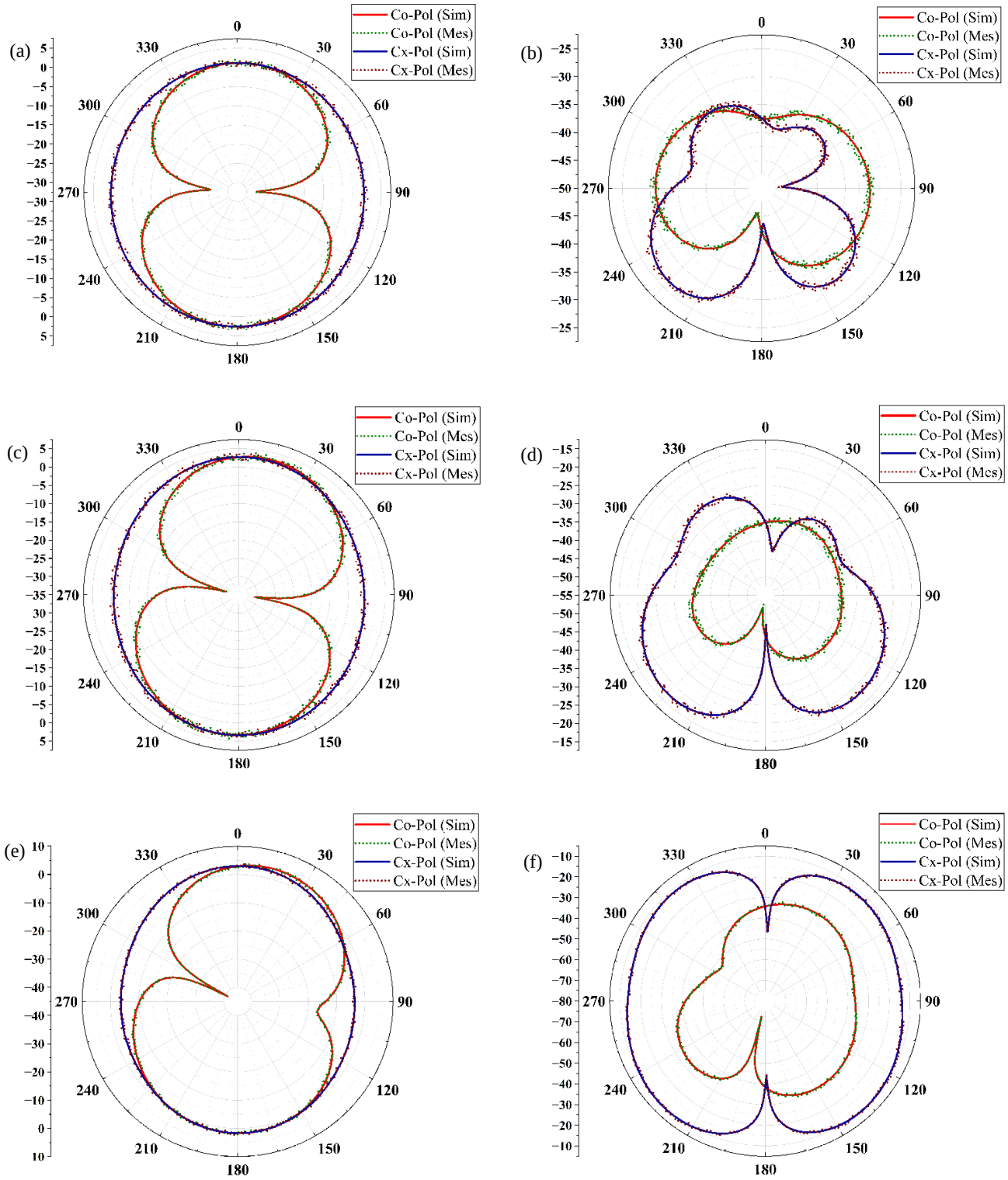

FIGURE 16. Designed antenna far-field radiation patterns: simulated & measured. (a) E-field at 4.2 GHz, (b) H-field at 4.2 GHz, (c) E-field at 5.7 GHz, (d) H-field at 5.7 GHz, (e) E-field at 6.9 GHz, (f) H-field at 6.9 GHz.

Figure 10 shows the compactness of the designed antenna, which is similar in dimension to a rupee coin with dimensions of 26 mm × 27 mm × 1.6 mm.

The fabricated MPA was tested in an anechoic chamber, as shown in Figures 11(a) and (b). The analysis examined the return loss, radiation pattern, gain, and Voltage Standing Wave Ratio (VSWR). Figure 11(c) depicts the measurement with Figure 11(c) depicts measurements with with Vector Network Anayzer (VNA).

Figures 12 and 13 illustrate a comparison of the simulated and measured S_{11} and VSWR values across the frequency spectrum. The results exhibited strong correlation and consistency.

The antenna successfully achieves a bandwidth of 3.39 GHz, spanning a frequency range of 3.57–6.96 GHz with a 64.39%

TABLE 2. Performance comparison of this compact design with reported compact designs in Sub-6 GHz range.

Ref.	Antenna Size	Substrate	Frequency Range (GHz)	Efficiency (∼%)	FBW (%)	Gain (Peak)
[1]	$0.34\lambda \times 0.34\lambda \times 0.02\lambda$	FR4	3.20–5.34	96%	50	2.76 dBi
[3]	$0.40\lambda \times 0.39\lambda \times 0.01\lambda$	FR4	3.4–4.3	43%	23.4	3 dBi
[4]	$0.71\lambda \times 0.81\lambda \times 0.016\lambda$	FR4	1.73–4.38	88–96%	86.7	5.1 dB
[5]	$0.18\lambda \times 0.31\lambda \times 0.007\lambda$	Rogers RT 5880	2.67–5.23 GHz	98%	Not reported	4.65 dB
[6]	$0.40\lambda \times 0.45\lambda \times 0.02\lambda$	FR4	3-7	Not reported	Not reported	∼3 dBi
[7]	$0.43\lambda \times 0.19\lambda \times 0.01\lambda$	FR4	3.3–4.0	Not reported	Not reported	∼2.5 dBi
[8]	$0.29\lambda \times 0.43\lambda \times 0.02\lambda$	FR4	3.15–5.55	68.4∼79.6	Not reported	1.87∼2.69 dBi
[9]	$0.59\lambda \times 0.24\lambda \times 0.006\lambda$	Teflon	2.32–5.24	Not reported	77.2	∼3 dB
[10]	$0.50\lambda \times 0.65\lambda \times 0.03\lambda$	Taconic TLY-5A	3.1–11.8	Not reported	Not reported	3.86 dBi
Present Work	$0.46\lambda \times 0.47\lambda \times 0.03\lambda$	FR4	3.57 to 6.96 GHz	89.2–95.46%	64.39%	4.8 dB

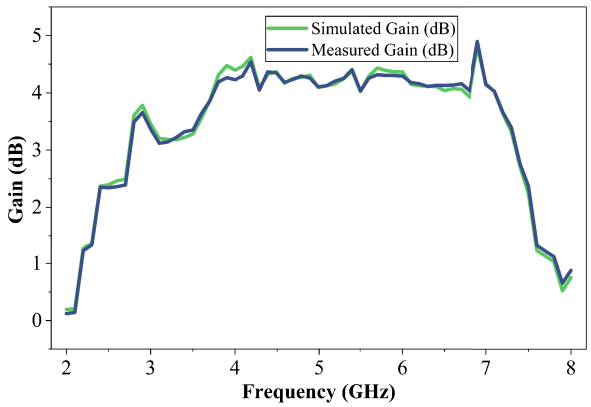

FIGURE 17. Simulated and measured gains of the designed antenna.

fractional bandwidth while maintaining an S_{11} value below -10 dB. Figure 14 shows that the radiation efficiency remains above 89% throughout the full 3.57–6.96 GHz band with a peak value reaching 95.46%. The total efficiency calculated as per Equation (8) remains above 80% throughout the full 3.57–6.96 GHz band with a peak value reaching 90.08%. As the proposed antenna exhibits good impedance matching over the operating band, the total efficiency closely follows the radiation efficiency.

Figure 15 illustrates the surface current patterns at 4.2, 5.7, and 6.9 GHz, showing how the antenna excites different resonant modes. The current began near the feed and gradually extended along the arms and edges, forming intricate paths. These variations suggest the activation of higher-order modes, thereby improving radiation characteristics. The increasing current strength and spread confirm the antenna's effective broadband operation and high efficiency.

As illustrated in Figure 16, the far-field radiation patterns of the proposed antenna are plotted for both the E-plane (XZ, $\Phi = 0°$) and the H-plane (YZ, $\Phi = 9°$) at 4.2, 5.7, and 6.9 GHz. In the XZ plane, the pattern reveals a clear bidirectional nature, which aids focused signal transmission. In contrast, the YZ plane shows a near-omnidirectional pattern, ensuring wider coverage and reliable performance.

Figure 17 shows a gain comparison of the designed antenna. For the entire band 3.57–6.96 GHz, sufficient gain is received with a maximum gain of 4.8 dB at 6.9 GHz frequency.

Table 2 provides a comparison between the performance of the designed antenna and other designs reported in the literature, assessing key parameters such as physical dimensions, gain, BW (%), substrate materials, frequency range, radiation efficiency, and feeding methods.

6. CONCLUSION

A compact wideband microstrip patch antenna that integrates a DGS and strategically placed slots was developed. By adding slot modifications to the structure, this antenna significantly improves the bandwidth while maintaining a small overall size of $26 \times 27 \times 1.6\,\text{mm}^3$ ($0.46\lambda \times 0.47\lambda \times 0.03\lambda$). Built on an FR4 substrate, this antenna works in the 3.57–6.96 GHz range with an S_{11} below -10 dB, making it usable for Sub-6 GHz, Wi-Fi, and WiMAX applications. The good match between the simulation and measurement verifies the design, with the antenna offering a maximum gain of 4.8 dB, a fractional bandwidth of 64.39%, and a high radiation efficiency of 95.46% while ensuring stable radiation across the frequency range. Owing to its small size, wide impedance bandwidth, and good performance, this antenna is an excellent choice for compact wireless devices, Internet of Things modules, and portable Sub-6 GHz communication systems.

ACKNOWLEDGEMENT

We would like to thank the Electromagnetics and Antenna Research Centre (ELARC Lab) at Birla Vishwakarma Mahavidyalaya, V. V. Nagar, Gujarat, India for providing measurement support.

REFERENCES

[1] Kapoor, A., R. Mishra, and P. Kumar, "Wideband miniaturized patch radiator for Sub-6 GHz 5G devices," *Heliyon*, Vol. 7, No. 9, e07931, Sep. 2021.

[2] Sun, K., Y. Tang, S. Liu, J. Pan, and D. Yang, "A wideband circularly polarized microstrip patch antenna with embedded shielding package based on quarter-mode substrate integrated waveguide feed," *IEEE Access*, Vol. 8, 140 524–140 532, 2020.

[3] Qian, L., X. Chen, X. Liu, H. Zhou, H. Wang, and M. Hou, "Low-profile wideband patch antenna using even and odd modes for 5G terminal applications," *IEEE Antennas and Wireless Propagation Letters*, Vol. 23, No. 8, 2476–2480, Aug. 2024.

[4] Prajapati, B. D., B. Jaiswal, and P. J. Dalvadi, "Wideband elliptical patch antenna integrating a circular notch and defected ground structure," *Progress In Electromagnetics Research C*, Vol. 156, 161–168, 2025.

[5] Paul, L. C., S. C. Das, T. Rani, S. M. Muyeen, S. A. Shezan, and M. F. Ishraque, "A slotted plus-shaped antenna with a DGS for 5G Sub-6 GHz/WiMAX applications," *Heliyon*, Vol. 8, No. 12, e12040, Dec. 2022.

[6] Farooq, U., M. Nasir, A. Iftikhar, M. S. Khan, A. Fida, M. F. Shafique, S. M. Asif, and R. M. Shubair, "A compact monopole patch antenna for future Sub 6 GHz 5G wireless applications," in *2020 IEEE International Symposium on Antennas and Propagation and North American Radio Science Meeting*, 1715–1716, Montreal, QC, Canada, Jul. 2020.

[7] Kapoor, A., R. Mishra, and P. Kumar, "Compact wideband-printed antenna for Sub-6 GHz fifth-generation applications," *International Journal on Smart Sensing and Intelligent Systems*, Vol. 13, No. 1, 1–10, Jan. 2020.

[8] Azim, R., A. M. H. Meaze, A. Affandi, M. M. Alam, R. Aktar, M. S. Mia, T. Alam, M. Samsuzzaman, and M. T. Islam, "A multi-slotted antenna for LTE/5G Sub-6 GHz wireless communication applications," *International Journal of Microwave and Wireless Technologies*, Vol. 13, No. 5, 486–496, Jun. 2021.

[9] Tang, X., Y. Jiao, H. Li, W. Zong, Z. Yao, F. Shan, Y. Li, W. Yue, and S. Gao, "Ultra-wideband patch antenna for Sub-6 GHz 5G communications," in *2019 International Workshop on Electromagnetics: Applications and Student Innovation Competition (iWEM)*, 1–3, Qingdao, China, Sep. 2019.

[10] Abbas, A., N. Hussain, J. Lee, S. G. Park, and N. Kim, "Triple rectangular notch UWB antenna using EBG and SRR," *IEEE Access*, Vol. 9, 2508–2515, 2021.

[11] Ali, T., M. S. Aw, R. C. Biradar, A. Andújar, and J. Anguera, "A miniaturized slotted ground structure UWB antenna for multi-band applications," *Microwave and Optical Technology Letters*, Vol. 60, No. 8, 2060–2068, Aug. 2018.

[12] Aravindraj, E., G. Nagarajan, and R. S. Kumaran, "A monopole octagonal Sierpinski carpet antenna with defective ground structure for SWB applications," in *Machine Learning, Deep Learning and Computational Intelligence for Wireless Communication*, Vol. 749, 267–280, E. S. Gopi (ed.), in Lecture Notes in Electrical Engineering, Springer, Singapore, 2021.

[13] Anguera, J., I. Sanz, A. Sanz, D. Gala, A. Condes, C. Puente, and J. Soler, "Enhancing the performance of handset antennas by means of groundplane design," in *IEEE International Workshop on Antenna Technology Small Antennas and Novel Metamaterials*, 29–32, White Plains, NY, USA, Mar. 2006.

[14] John, D. M., S. Vincent, S. Pathan, P. Kumar, and T. Ali, "Flexible antennas for a Sub-6 GHz 5G band: A comprehensive review," *Sensors*, Vol. 22, No. 19, 7615, Oct. 2022.

[15] Singh, A. and S. Joshi, "Design of Y-shaped tri-band rectangular slot DGS patch antenna at Sub-6 GHz frequency range for 5G communication," *Journal of Engineering and Applied Science*, Vol. 71, No. 1, 144, 2024.

[16] Abbas, A., N. Hussain, M. A. Sufian, W. A. Awan, J. Jung, S. M. Lee, and N. Kim, "Highly selective multiple-notched UWB-MIMO antenna with low correlation using an innovative parasitic decoupling structure," *Engineering Science and Technology, an International Journal*, Vol. 43, 101440, Jul. 2023.

[17] Elabd, R. H., A. J. A. Al-Gburi, and A. A. Megahed, "Compact circular MIMO antenna with defected ground structure (DGS) for improved isolation in 5G Sub-6 GHz mobile systems," *Results in Engineering*, Vol. 27, 105737, Sep. 2025.

[18] Saeidi, T., A. J. A. Al-Gburi, and S. Karamzadeh, "A miniaturized full-ground dual-band MIMO spiral button wearable antenna for 5G and Sub-6 GHz communications," *Sensors*, Vol. 23, No. 4, 1997, Feb. 2023.

[19] Azim, R., R. Aktar, A. K. M. M. H. Siddique, L. C. Paul, M. T. Islam, *et al.*, "Circular patch planar ultra-wideband antenna for 5G Sub-6 GHz wireless communication applications," *Journal of Optoelectronics and Advanced Materials*, Vol. 23, 127–133, 2021.

[20] Tiwari, P. and P. K. Malik, "Design of UWB antenna for the 5G mobile communication applications: A review," in *2020 International Conference on Computation, Automation and Knowledge Management (ICCAKM)*, 24–30, Dubai, United Arab Emirates, Jan. 2020.

[21] Khan, M. S., A. Iftikhar, R. M. Shubair, A.-D. Capobianco, B. D. Braaten, and D. E. Anagnostou, "Eight-element compact UWB-MIMO/diversity antenna with WLAN band rejection for 3G/4G/5G communications," *IEEE Open Journal of Antennas and Propagation*, Vol. 1, 196–206, 2020.

[22] Jha, K. R., Z. A. P. Jibran, C. Singh, and S. K. Sharma, "4-Port MIMO antenna using common radiator on a flexible substrate for Sub-1 GHz, Sub-6 GHz 5G NR, and Wi-Fi 6 applications," *IEEE Open Journal of Antennas and Propagation*, Vol. 2, 689–701, 2021.

[23] Saeidi, T., S. N. Mahmood, S. Alani, S. M. Ali, I. Ismail, and A. R. H. Alhawari, "Sub-6G metamaterial-based flexible wearable UWB antenna for IoT and WBAN," in *2020 IEEE Intl. Conf. on Dependable, Autonomic and Secure Computing, Intl. Conf. on Pervasive Intelligence and Computing, Intl. Conf. on Cloud and Big Data Computing, Intl. Conf. on Cyber Science and Technology Congress (DASC/PiCom/CBDCom/CyberSciTech)*, 7–13, Calgary, AB, Canada, Aug. 2020.